THEORETICAL & APPLIED MECHANICS LETTERS **3**, 032008 (2013)

Fluid flow in charged nanotubes

Xiaofeng Yang,[1, a)] Mei Feng,[2] Yanyan Chen,[2] Hangjun Lu,[2] and Xiaoyan Zhou[2, 3, b)]
[1)] *Electromechanical and Informational Institute, Yiwu Industrial and Commercial College, Yiwu 322000, China*
[2)] *Department of Physics, Zhejiang Normal University, Jinhua 321004, China*
[3)] *Department of Physics and Institute of Theoretical Physics, Shanxi University, Taiyuan 030006, China*

(Received 26 February 2013; accepted 25 March 2013; published online 10 May 2013)

Abstract The dynamics of fluid flow through nanochannels is different from those in macroscopic systems. By using the molecular dynamics simulations, we investigate the influence of surface polarity of nanotube on the transport properties of the water fluid. The nanotube used here resembles the carbon nanotube, but carries charges of q on some atoms; overall, the nanotube is charge-neutral. Our simulation results show that water flux decreases sharply with the increasing of q for $q < 1.6$ e; however, the water flux for shells far away from nanotube wall increases slightly when $q > 1.6$ e. The mechanism behind the interesting phenomenon is discussed. Our findings may have implications for development of nano-fluidic devices and for understanding the movement of confined fluid inside the hydrophilic nanochannel. [doi:10.1063/2.1303208]

Keywords nano fluid, molecular dynamics, hydrophilic nanotube, transport

Shale gas, natural gas formed from being trapped within shale formations, has become an increasingly important source of natural gas in the world. Some analysts expect that shale gas will greatly expand worldwide energy supply.[1] China is estimated to have the world's largest shale gas reserves.[2] Nanoscale pores were found in shale gas reservoirs by Howard[3] and Sondergeld et al.[4] The presence of nanoscale pores in the shale gas makes it considerable to study the behavior of fluid in those very small pores. Interest in understanding the movement of small volumes of fluid has been growing rapidly in recent years.[5] Understanding the flow of liquids through nano pipes is also of great importance for designing novel molecular machines, sensors and nano-fluidic devices.[6–17] Models of fluid behavior in pipe with a diameter on the order of inches or feet usually begin with continuum hypothesis, where the atomic structure of fluid is ignored and the fluid is instead characterized by viscosity, density, and other bulk properties.[16,18] Interestingly, the behavior of fluids confined in nanomachines is expected to be fundamentally different from bulk behavior, as the characteristic dimension of the confining volume reduces to the nanometer scale. Microscopic fluctuations play a key role, and it no longer makes sense to describe the permeant fluid as a continuum.[19–24]

Carbon nanotubes are molecular-scale tubes of graphitic carbon with outstanding properties and potentials for applications in nanoscale sensors, fluid filtration, targeted drug delivery devices and machines.[25,26] Because of their exceptional mechanical and thermal stability, nanotubes are also ideal candidates as cavities for chemical reactions at high temperatures and pressures.[27,28] In 2001, by using molecular dynamics, Hummer et al.[29] found that a (6, 6) nonpolar carbon nanotube 1.34 nm long with a diameter of 0.81 nm can be filled with water in spite of its strongly hydrophobic character. Recently, both experimental and theoretical studies have demonstrated that the confinement of water inside a carbon nanotube can lead to interesting structures and behavior not seen in the bulk, such as the ordered water structure,[30–32] non-Fickian-type diffusion,[33] and extra fast motion of water fluid.[34]

Water behavior in nanochannels relies on the structure of water layers close to the surface of the channels. And water layers near the surface often exhibit unique properties. Ice-like water monolayers on mica, mental surfaces were found, which have longer relaxation time when compared to bulk liquid water.[35,36] Recent study of water adsorbed on mental surfaces demonstrated that ice-like monolayers have hydrophobic-like property due to the fact that no dangling OH bonds exist in the ice-like monolayer, which itself features a two-dimensional hydrogen bond network.[36–39] Several factors, such as temperature, surface roughness and surface polarity, could affect the wetting behavior of water molecules on surfaces. In particular, surface polarity has been recognized as playing a crucial role in determining the behavior of water at hydrated interfaces. Fang's group,[40] using molecular dynamics simulations, demonstrated that "water does not wet a water monolayer" (i.e., hydrophobic water layer) at room temperature, which was also observed by experiments. The substrate in Ref. 40 has a planar hexagonal structure of neighboring bond lengths of 0.142 nm, which is similar to the graphene surface.

In this paper, the same substrate as in Ref. 40 is rolled up into a charged nanotube. We devoted to study how the charged surfaces of the nanotube affect the properties of inner water layers. This discovery has significant implications, both for our understanding of how fluids behave at very small length scales and for the design of nano-fluidic devices.

Figure 1 shows the simulation framework, in which the (40, 40) charged carbon nanotube with 5.346 nm

[a)] Email: xfy1970@zjnu.cn.
[b)] Corresponding author. Email: zxylu@zjnu.cn.

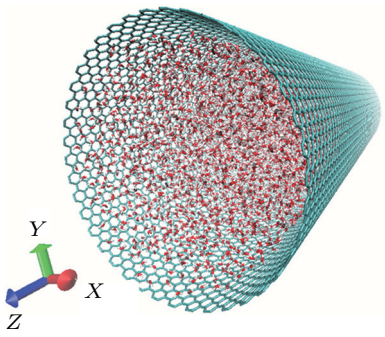

(a) Schematic of water fluid flowing through a charged nanotube

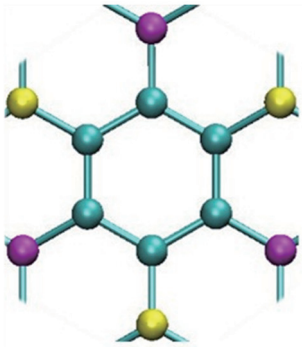

(b) Geometry of the nanotube model. Yellow and purple spheres represent negative and positive charges, respectively, while the green represents the neutral solid atom

Fig. 1. Simulation framework.

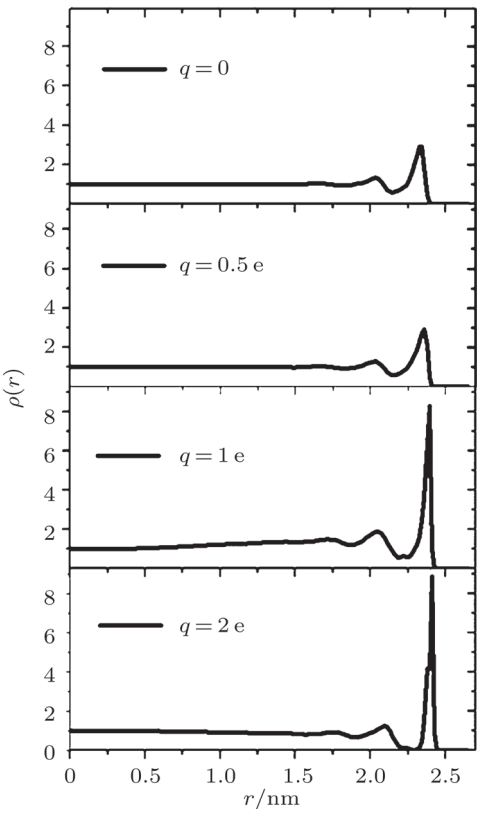

Fig. 2. Radial density profiles of the water in the nanotubes for different q. r is the distance from the center of the nanotube.

diameter is filled with 4 572 water molecules. The simple point charge/extended simple point charge (SPC/E) water model was used. Positive and negative charges of the same magnitude q were assigned to atoms located diagonally in neighboring hexagons (see Fig. 1(b)). It should be noted that this is just a model system with relatively large charges for simulation purpose. Overall, the modeled nanotube is charge-neutral.

Our simulations were performed at a constant molecule number, volume and temperature, using a time step 2.0 fs (1 fs = 10^{-15} s) with the Gromacs 4.0.7.[41] The temperature was maintained at 300 K using Nose–Hoover thermostat. The Lennard–Jones parameters for the interaction among the carbon atoms are ε_{cc} = 0.105 kcal/mol (1 kcal = 418 6 J), σ_{cc} = 3.343 Å (1 Å = 10^{-10} m). In addition, the carbon-water interactions are σ_{co} = 0.327 53 nm and ε_{co} = 0.119 86 kcal/mol. A periodic boundary condition was applied in the axial direction (z) and the simulation box size was 10 nm×10 nm×7.518 nm. The cutoff distance for the Lennard–Jones interactions is 15 Å. The long-range electrostatic interactions were computed by using the particle mesh Ewald method (real space cutoff, 10 Å; reciprocal space gridding, 1.2 Å, the fourth-order interpolation). Similar to previous works, the carbon atoms were frozen to their lattice position.[33,42–44] According to the method in Ref. 45, a pressure gradient to drive water fluid was offered by adding an additional acceleration of 0.01 nm/ps^2 (1 ps = 10^{-12} s) to each water molecule along the $+z$ direction.[45]

The radial density profiles of the water in the nanotube with different q are calculated, shown in Fig. 2. Here, the radial density $\rho(r)$ is defined as the ratio of local water fluid density at r to the water fluid density at the center region of the nanotube. The local densities are calculated by dividing the water fluid into many cylindrical shells in the r direction, then taking the average for the density for each shell. From Fig. 2, we can see that there is a sharp density peak near the nanotube wall due to the attractive interaction between the water and the wall of the nanotube. However, in the center region of the nanotubes, the water molecule distributions are uniform, which is similar to the bulk water. As the charge q assigned to the nanotube increases, the first density peak close to the wall becomes sharper and sharper. We can conclude that the first water monolayer near the tube wall becomes more and more ordered. Correspondingly, the diffusion constant of water layers close to the wall decreases. Due to the strong Coulomb force between the charged wall and water dipoles, the water layers shifts toward to the tube wall slightly as well. According to the distribution of water density, the inner confined water molecules can be divided into four shells. The region sizes of the 1st, 2nd and 3rd shell are about the size of one water molecule

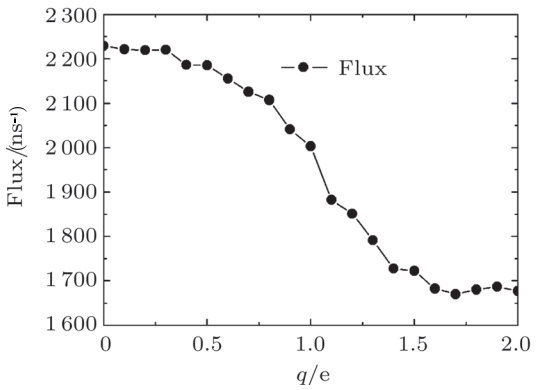

Fig. 3. Water flux through the charged nanotube for different q.

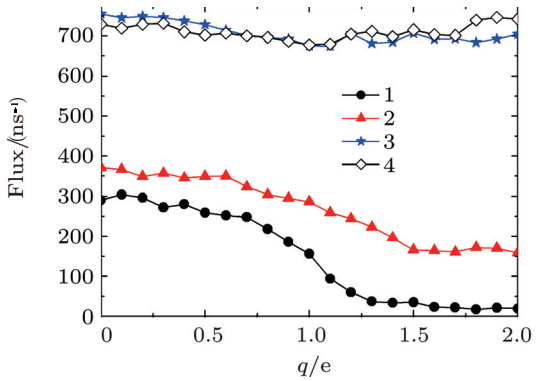

Fig. 4. Flux through the charged nanotube for different shells.

(about 3.8 Å), while the fourth shell, considered as bulk shell, is much larger.

For easy discussion, we define flux as the difference between the number of water molecules per nanosecond leaving from one end to the other of the nanotube.[46] Figure 3 displays the water flux through the charged nanotube for different q. For the uncharged nanotube ($q = 0$), the water flux is about 2 229 ns^{-1}. It decreases sharply with q when $q < 1.6$ e due to the attractive interaction between the water molecules and the charged wall. Though the Coulomb forces between the water molecules and the charged wall of the nanotube increase with q, the water flux almost keep constant (about 1 677 ns^{-1}) when $q > 1.6$ e.

In order to understand the mechanism, we calculated the water flux for different shells. For uncharged nanotube, water flux for the 1st, 2nd, 3rd and 4th shell is 290 ns^{-1}, 371 ns^{-1}, 755 ns^{-1} and 729 ns^{-1}, respectively. The water flux for the 1st and 2nd shell decreases clearly with q, however the water flux for the 3rd and 4th shell decreases slightly when $q < 1.6$ e. It is remarkable to find that the water flux for the 3rd and 4th shells increases slightly when q increases further. Then how to explain this unexpected increase in the water flux for the 3rd and 4th shells? We have found that the ordered first water monolayer near the charged

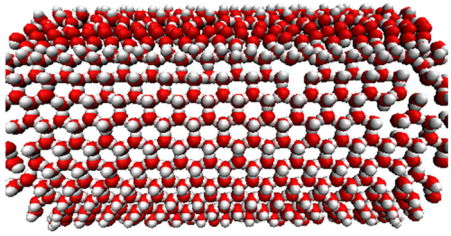

Fig. 5. Hexagonal ice monolayer of first layer formed near the charged nanotube wall.

wall of the nanotube is responsible for this abnormal flow. Here, a hexagonal ice monolayer is formed near the charged nanotube wall (shown in Fig. 5), which affects the dynamic of fluid flow inside the nanotube.

By virtue of molecular dynamics simulation, we studied the transport of the water fluid through the charged nanotube. We find that there is a sharp peak in the radial density of water close to the wall of the nanotube. And it moves to the charged wall when charge value q increases. Correspondingly, water flux for the first and second shell decreases sharply with q. Interestingly, the water flux for the 3rd and 4th shell increases slightly when $q > 1.6$ e. And we also find a hexagonal ice monolayer close to the wall correspondingly. These findings may be helpful in designing nano-fluidic devices and in understanding the behavior of confined fluid in hydrophilic nanochannel. Another phenomenon we should not neglect is that there is a smaller peak next to the sharp peak of the first layer (i.e. the second shell) and that the water flux for the third, fourth shell increases slightly.

The authors would like to thank Haiping Fang, Chunlei Wang, and Junxia He, for helpful discussions. This work was partially supported by the National Natural Science Foundation of China (11005093,10932010, 11072220, 11072229, U1262109, 51176172, and 10972208), the Zhejiang Provincial Natural Science (Z6090556, Y6100384), and Project of Educational Department of Zhejiang Province (Y200909221).

1. C. Krauss, *New way to tap gas may expand global supplies*, New York Times, 9 October 2009.
2. *World shale gas resources: An initial assessment of 14 regions outside the United States*, US Energy Information Administration, http://www.eia.gov/analysis/studies/worldshalegas.
3. J. J. Howard, Clays and Clay Minerals **39**, 4 (1991)
4. C. H. Sondergeld, R. Ambrose, and C. S. Jrai, *Micro-Structural Studies of Gas Shales*. In: Proceedings of SPE Unconventional Gas Conference, Pittsburgh, Pennsylvania, USA (2010).
5. A. B. D. Brown, C. G. Smith, and A. R. Rennie, Phys. Rev. E **63**, 016305 (2000).
6. J. Su, and H. Guo, J. Phys. Chem. B **116**, 5925 (2012).
7. H. Lu, X. Nie, and F. Wu, et al., J. Chem. Phys. **136**, 174511 (2012).
8. Y. C. Zhao, L. Song, and K. Deng, et al., Advance Materials **20**, 1772 (2008).

9. H. A. Zambrano, J. H. Walther, and P. Koumoutsakos, et al., Nano Lett. **9**, 66 (2008).
10. A. Noy, H. G. Park, and F. Fornasiero, et al., Nano Today **2**, 22 (2007).
11. G. M. Whitesides, Nature **442**, 368 (2006).
12. Z. Insepov, D. Wolf, and A. Hassanein, Nano Lett. **6**, 1893 (2006).
13. T. M. Squires, and S. R. Quake, Rev. Mod. Phys. **77**, 977 (2005).
14. Y. C. Liu, and Q. Wang, Phys. Rev. B **72** (2005).
15. B. Huang, Y. Xia, and M. Zhao, et al., J. Chem. Phys. **122**, 084708 (2005).
16. V. P. Sokhan, D. Nicholson, and N. Quirke, J. Chem. Phys. **115**, 3878 (2001).
17. R. E. Tuzun, D. W. Noid, and B. G. Sumpter, et al., Nanotechnology **7**, 241 (1999).
18. M. M. Denn, *Process Fluid Mechanics* (Prentice-Hall Englewood Cliffs, NJ, 1980).
19. L. D. Gelb, and K. E. Gubbins, Rep. Prog. Phys. **63**, 727 (2000).
20. T. M. Truskett, Proc. Natl. Acad. Sci. USA **100**, 10139 (2003).
21. X. Y. Zhou, and H. J. Lu, Chin. Phys. **16**, 335 (2007).
22. P. Xiu, Y. S. Tu, and X. L. Tian, et al., Nanoscale **4**, 652 (2012).
23. C. L. Wang, B. Zhou, and Y. S. Tu, et al., Scientific Reports **2**, 358 (2012).
24. P. Xiu, B. Zhou, and W. P. Qi, et al., Journal of The American Chemical Society **131**, 2840 (2009).
25. S. Iijima, Nature **354**, 56 (1991).
26. X. J. Gong, J. Y. Li, and H. J. Lu, et al., Nature Nanotechnology **2**, 709 (2007).
27. M. Longhurst, and N. Quirke, Nano Lett. **7**, 3324 (2007).
28. X. Pan, Z. Fan, and W. Chen, et al., Nat. Mater. **6**, 507 (2007).
29. G. Hummer, J. C. Rasaiah, and J. P. Noworyta, Nature **414**, 188 (2001).
30. K. Koga, G. T. Gao, and H. Tanaka, et al., Nature **412**, 802 (2001).
31. R. J. Mashl, S. Joseph, and N. R. Aluru, et al, Nano Lett. **3**, 589 (2003).
32. N. Giovambattista, P. J. Rossky, and P. G. Debenedetti, Phys. Rev. E **73**, 14 (2006).
33. A. Striolo, Nano Lett. **6**, 633 (2006).
34. J. K. Holt, H. G. Park, and Y. M. Wang, et al., Science **312**, 1034 (2006).
35. S. H. Park, and G. Sposito, Phys. Rev. Lett. **89**, 085501 (2002).
36. S. Meng, E. G. Wang, and S. Gao, Phys. Rev. B **69**, 195404 (2004).
37. C. Wang, H. Lu, and Z. Wang, et al., Phys. Rev. Lett. **103**, 137801 (2009).
38. G. A. Kimmel, J. Matthiesen, and M. Baer, et al., J. Am. Chem. Soc. **131**, 12838 (2009).
39. G. A. Kimmel, N. G. Petrik, and Z. Dohnálek, et al., Phys. Rev. Lett. **95**, 166102 (2005).
40. C. Wang, J. Li, and H. Fang, Earth and Environmental Science **22**, 1 (2011).
41. B. Hess, C. Kutzner, and D. van der Spoel, et al., Journal of Chemical Theory and Computation **4**, 435 (2008).
42. A. Barati Farimani, and N. R. Aluru, J. Phys. Chem. B **115**, 12145 (2011).
43. E. M. Kotsalis, J. H. Walther, and P. Koumoutsakos, Int. J. Multiphase Flow **30**, 995 (2004).
44. A. Striolo, A. A. Chialvo, and K. E. Gubbins, et al., J. Chem. Phys. **122**, 234712 (2005).
45. F. Q. Zhu, and K. Schulten, Biophys. J. **85**, 236 (2003).
46. X. Gong, J. Li, and H. Zhang, et al., Phys. Rev. Lett. **101**, 257801 (2008).